THERMAL RESPONSE AND ABLATION CHARACTERISTICS OF QUARTZ-PHENOLIC AND CARBON-PHENOLIC COMPOSITES

Edson de Aquino Barros, barros@ita.br
Gilberto Petraconi Filho, gilberto@ita.br
Instituto Tecnológico de Aeronáutica - São José dos Campos SP
Maria Luisa Gregori, luisa.gregori@iae.cta.br
Instituto de Aeronáutica e Espaço - São José dos Campos SP
Sonia Fonseca Costa e Silva, sonia@iae.cta.br
Instituto de Aeronáutica e Espaço - São José dos Campos SP
Leonid Ivanovich Charakhovski, leonidsh@tu.by
Homero Santiago Maciel, homero@ita.br
Instituto Tecnológico de Aeronáutica - São José dos Campos SP

Abstract. This work present the thermal response and ablation characteristics of quartz-phenolic and carbon-phenolic composites used in thermal protection systems for aerospace purposes. These materials were exposed to a plasma jet with thermal fluxes similar to those encountered in atmospheric reentry vehicles. The tests was done in a reactive air plasma, using a DC non transferred arc plasma torch, with enthalpies from 6.2MJ/kg to 9.4MJ/kg, corresponding to thermal fluxes from 0.52MW/m^2 to 2.2 MW/m^2. The mass loss, the ablation heat, the superficial radiometric and internal temperatures were evaluated as a function of the exposure time and heat flux. Additionally, was evaluated the mass loss behavior as a function of temperature by thermo gravimetric analyses. The micro structural aspects were investigated by Scanning Electron Microscopy (SEM). A more complete and detailed characterization was carried out for the quartz-phenolic, due to the fact that this material was developed and fabricated in Brazil, having a special interested for the Aeronautical and Space Institute. The results show that the quartz-phenolic composites have the highest ablation heat, more than twice the value obtained for the other tested materials. The carbon-phenolic composites show almost the double of the value for the mass loss comparing to the quartz-phenolic. This is due to the higher conductivity of the carbon fibers (11W/mK), in comparison to the quartz fibers (1.5W/mK), leading to an increase in the volatilization of resin in the carbon composites. The SEM analyses of the quartz-phenolic show that there was fusion of the superficial layer of the fibers of quartz-phenolic composite, because the melting temperature of the quartz is around 1500 ^{o}C, temperature that was reached during the test as results of the pyrometer measurements. Quartz fibers melting implies in a loss of mechanical strength of reinforcement composite. Therefore, in regions subject to mechanical strain, should consider the use of carbon fiber because of its melting temperature is around 3000 ^{o}C, temperatures well above those planned to be achieved during the reentry of an orbital vehicle. *A general analysis of the results with the focus in the optimization of a thermal plasma torch apparatus for the investigation of the ablative process of materials used in thermal protection systems and nozzles shows the viability to open a research field, up to now not available in Brazil, in order to qualify and certify materials for aerospace industry.*

Keywords*: heat of ablation, composite, atmospheric reentry*)

1. INTRODUCTION

Polymer composites are widely used for high temperature thermal protection (TPS) materials. Such kinds of composites are often called as ablative material or ablator. Ablative materials are utilized for spacecraft heat shields for atmospheric re-entry, and rocket nozzle liners of solid propellant rocket motor (Ogasawara and Ishikawa, 2002).

They are often subjected to the combinations of lateral pressure and thermal loading. Composite structures have high stiffness, strength and fatigue properties. Degradation of physical properties by various environmental free and force effects such as temperature and pressure load is very important factor in prediction the durability of composite materials (Bahramian et al, 2006).

Thermal degradation of polymer and composite structures is a complex phenomenon and a great deal of research is performed on this subject. The thermal degradation of a composite covers a wide field of important processes such as the development of heat resistant, thermal stabilization, and the characterization of high-temperature composites for aircraft and aerospace usage.

Generally, the thermal degradation of a polymeric composite follows more than one mechanism, the existence of various concurrent chemical reactions accompanied by other physical phenomena such as sublimation; melting and ablation introduce further complication for the modeling of the degradation kinetics.

Ablation is an effective and reliable method largely used in aerospace structures to protect the pay load from the damaging effects of external high temperatures. In the ablation process, the high-heat fluxes are dissipated by the material through a series of endothermic processes. That finally led to the loss and the consumption of the material itself. The working process of an ablative heat shield can be briefly summarized as follows; the convective heat that reaches to the vehicle surface is balanced by surface radiation, phase transitions, and chemical reactions. Moreover, part of the incoming convective heat flux is blocked by the out coming flow of hot gases that result from the degradation processes. The ablative material keeps the surface temperature within a certain range and as a consequence an increase of the heat flux will not cause a consistent temperature raise, but will cause an increase of the surface recession rate.

1.1. Heat of ablation.

The heat of ablation provides a measure of the ability of a material to serve as a heat protection element in a severe thermal environment. In general, it is defined as the incident heat dissipated by the ablative material per unit of mass removed. The property is a function of both the material and the environment to which it is subjected. It is therefore required that laboratory measurements of heat of ablation simulate the service environment as closely as possible. Some of the parameters affecting the property are pressure, gas composition, heat transfer rate, mode of heat transfer, and gas enthalpy. As laboratory duplication of all parameters is usually difficult, the user of the data should consider the differences between the service and the test environments. Screening tests of various materials under simulated use conditions may be quite valuable even if all the service environmental parameters are not available. These tests are useful in material selection studies, materials development work, and many other areas (Schmidt, 1971).

1.2. Eart Entry.

Heating during atmospheric entry depends on the trajectory, which is a function of the vehicle configuration and weight as well as its initial entry angle and speed. Taking as example, a satellite in orbit at 300 km altitude, one can easily estimate a circular velocity using the Eq. (1) (Regan, 1993):

$$V_{circular} = \sqrt{\frac{GE}{R_e + h}} = 7{,}73 km/s \tag{1}$$

Earth gravitational parameter (GE = 398600 km^3/s^2), earth radius (R_e = 6378 km), altitude (h = 300 km).

Assuming that this satellite begins a process of reentry and that the kinetic energy (E_k) dissipated in the process of deceleration is converted into heat (Q) result Eq. (2):

$$\frac{Q}{m} \cong \frac{E_k}{m} = \frac{1}{2} V_{circular}^2 = 30 MJ/kg \tag{2}$$

Q = quantity of heat, E_k = kinetic energy, m = mass of the satellite.

The heat flux of atmospheric reentry of a vehicle in orbit, to altitude of 300 km, which defines a circular velocity using equation (1), is a function of re-entry angle (θ) and the coefficient of drag vehicle (C_D). Figure 1 show the predicted aerothermodynamics environment for the stagnation region which was calculated by analytical techniques described by Fay and Riddell (1958) as function of atmospheric reentry time running after start of significant heat flux.

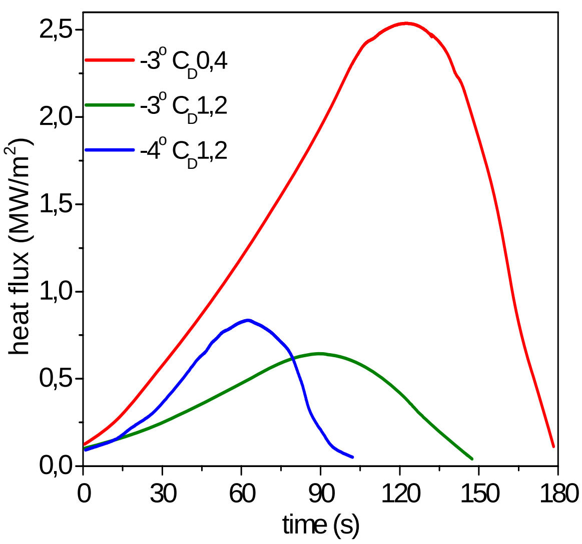

Figure 1. Heat flux of orbit vehicle atmospheric reentry for 300 km altitude, re-entry angle (θ) and drag coefficient (C_D).

2. MATERIALS AND METHODS.

2.1. Experimental setup.

To reproduce the heat flow to test the heat of ablation of composite samples of quartz-phenolic and carbon-phenolic has been used a plasma torch developed in the Technological Institute of Aeronautics (ITA) (Charakhovski et al 2008).

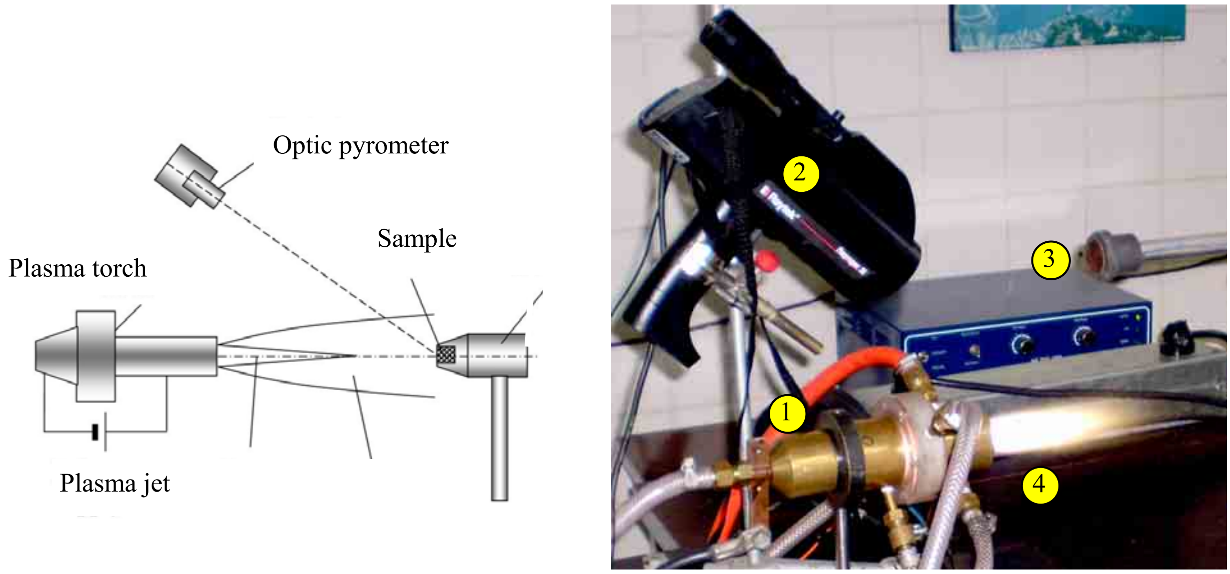

Figure 2. Main components of experimental setup: (1) plasma torch, (2) pyrometer, (3) sample-hold, (4) plasma jet.

2.2. Plasma torch.

The plasma torch (Fig. 2) is used to generate the intense heat flow (~ 2 MW/m^2) that is necessary to test samples of materials for thermal protection. The plasma jet is produced through Arc electric discharge that is generated in the air flow injected inside of the torch electrodes. Through the Arc discharge the air is ionized and the electric power is converted into heat energy. The condition set as standard for operation of the plasma torch and testing of samples of material ablation of thermal protection has the following parameters: current 90A, voltage 345V, air mass flow 3.1 g / s.

2.3. Quartz-phenolic and carbon-phenolic samples.

The samples of composite quartz-phenolic and carbon-phenolic which were developed in the CTA, in the period 2007 to 2008, were prepared in the workshop of the Department of Physics of the ITA, and cut with standard diameter of 30 mm, as shown in Fig. 3. To measure the internal temperature variation over the samples, thermocouples were inserted at 2 mm and 4 mm deep with respect to front face exposed to the plasma jet.

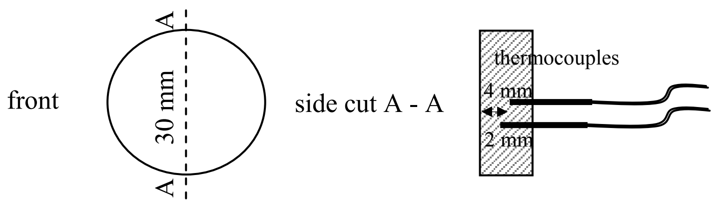

Figure 3. Samples setup diagram with positioning of thermocouples.

3. CHARACTERIZATION METHODS.

3.1. Measuring the samples temperature.

The samples internal temperatures were measured by using thermocouples "type k" inserted a 2 mm and 4 mm deep. The radiometric surface temperature was measured by an optical pyrometer, model Raytek 3i 1M, which measures temperatures in the range of 600 ^{o}C to 3000 ^{o}C, with resolution of 1^{o}C and accuracy of 0.05%.

3.2 Measuring the plasma jet heat flow.

A cold wall calorimeter exposed under same samples test conditions are subject was used to measure the heat flow produced by plasma jet (q_{cw}). Assuming that the copper cold wall is completely catalyst by providing the recombination of ionized particles of gas and 100% absorption of the incident heat, the amount of heat ($Q=mc_p\ \Delta T$) that enters a calorimeter represent the heat flow (q_{cw}) incident on the surface area of the calorimeter, due to all the processes of heat transfer.

Measures the rate of heat transfer through the method of the transient is obtained by measuring the rate of rise of temperature of a small disc of copper, at room temperature (~ 300 K), whose front surface is suddenly exposed to the plasma jet for a short period of time (~ s). Assuming that the flow of heat applied is constant, a first-order approximation, the response of temperature versus time will be given by Eq. (3):

$$T - T_0 = \dot{q}\tau / \rho c_p \delta \tag{3}$$

T_0 initial temperature (K); q_{cw} cold wall heat flux (W/m^2), τ exposition time (s), ρ density (kg/m^3), c_p specific heat (J/kg.K), *and* δ thickness of calorimeter;

As it is difficult to determine the temperature and the exact moment when the calorimeter is exposed to the jet of plasma is made using the derivative of Eq. (3):

$$\dot{q}_{cw} = \rho \delta c_P \frac{dT}{d\tau} \tag{4}$$

The calorimeter used (Fig. 4) consists of a copper disk (diameter 10.0 mm, thick 1.30 mm), which was set in a cylindrical holder made of low thermal conductivity material (2W/mK) compared to copper (398W/mK).

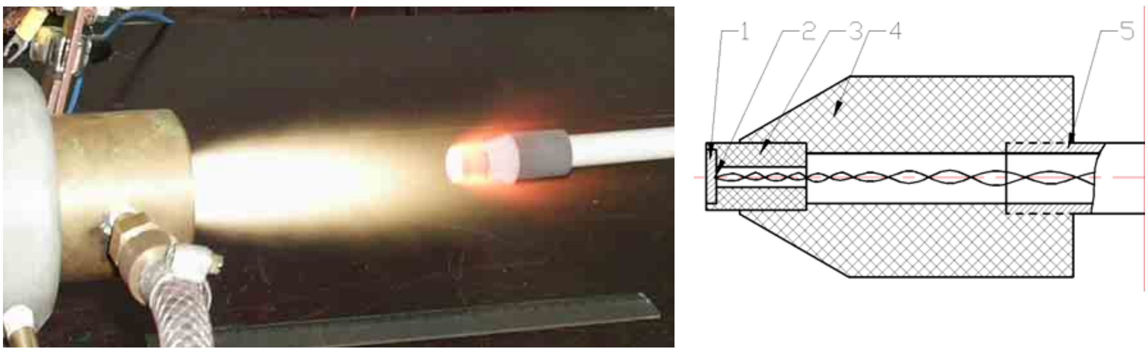

(a) (b)

Figure 4. (a) Calorimeter exposed to the plasma jet. (b) Schematic: 1 copper, 2 thermocouple, 3, 4 insulating, 5 support.

3.3. Cold-wall heat of ablation.

The cold-wall heat of ablation (Q_{cw}) of samples material tested was calculated by the incident cold-wall heat (q_{cw}) dissipated by the ablative material per unit of mass removed ($\dot{m}$), as follows Eq. (5):

$$Q_{cw} = q_{cw} / \dot{m} \tag{5}$$

3.4. Determination of Mass-Transfer Rate.

The determination of the heat of ablation requires the measurement of the mass-transfer rate of the material under test. This may be accomplished in several ways depending on the type of material under test. The heat of ablation value can be affected by the choice of method. We use the direct weighing method to determining mass-transfer rate, by the use of a pretest and post-test mass measurement. This procedure yields the mass transfer rate directly. In this method the mass-transfer rate is averaged over the entire test model heated area, and is also averaged over the insertion period.

The mass-transfer rate ($\dot{m}$) of the material area (πr^2) exposed under test was determining by pretest and post-test mass difference (Δm) and plasma jet exposition time (t_{ej}), as follows Eq. (6):

$$\dot{m} = \frac{\Delta m / \pi r^2}{t_{ej}} \tag{6}$$

3.5. Thermogravimetric Analysis (TGA).

Thermogravimetric analyses (TGA) were performed to characterize the percentage of loss of weight of samples of composites of thermal protection tested. The TGA tests were performed in a thermogravimetric analyzer, model Netzsch TG 209 F1 Iris. The samples were placed in door-sample of alumina (Al-203), under nitrogen atmosphere (25 ml/min), and heated from ambient temperature to 900 ^{o}C, 15 ^{o}C/min.

4. EXPERIMENTAL RESULTS.

4.1. Thermogravimetric Analysis (TGA) results.

Since the fibers of quartz and carbon does not suffer change in mass when heated to maximum temperature (900^{o}C), in inert atmosphere (N_2), which made the TGA analysis, it was determined the amount of resin lost the samples. The variation in the rate of mass loss observed in TGA is related to the type of fiber reinforcement of the matrix and also the percentage of phenolic resin used in the manufacture of the composite.

Figure 5 shows the TGA plot for quartz-phenolic composites and carbon-phenolic tested. Comparison of these results it appears that only the initial loss of mass is slightly different depending on the thermal conductivity of fiber reinforcement used. In composites reinforced with carbon fibers, with higher thermal conductivity (11 W/mK), the loss of initial mass is greater than in reinforced with a quartz fiber, with lower thermal conductivity (1.5 W/mK). As these composites have the same initial concentrations of phenolic resin (42%), the final percentage of solid waste is the same (78%), regardless of the type of fiber reinforcement used.

In TGA first derivative graph of composites there is a top temperature of the volatilization of phenolic resin (400 ^{o}C), the temperature in which the maximum rate of weight loss (540 ^{o}C) and the temperature of termination of volatilization and carbonization of the phenolic resin (800 ^{o}C).

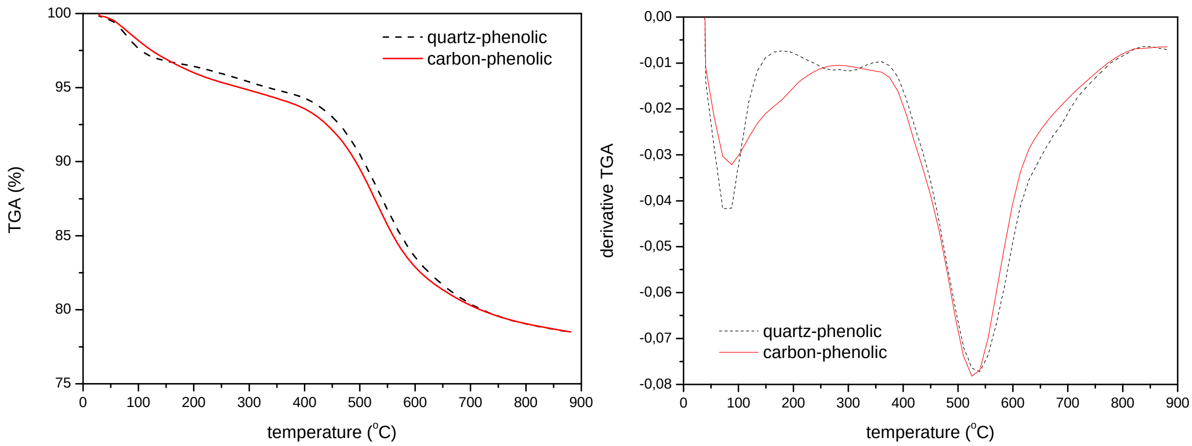

Figure 5. Thermogravimetric analyses (TGA) of composites quartz-phenolic and carbon-phenolic.

4.2. Characterization of the plasma jet.

To determine the heat of ablation of the composite is necessary to determine the rate of mass loss of samples depending on the intensity of the heat flux incident. Therefore it is necessary to characterize the intensity of the jet produced by plasma torch according to the position. The flow of heat produced by the plasma jet was measured with a calorimeter of cold wall using the method of analysis of transient temperature (expression 4).

Table 1 shows data used to calculate the intensity of the heat flux using the first derivative of the curve of temperature of the calorimeter as a function of exposure time to the plasma jet at the point with temperature equal to

350 K and considering the following properties of the copper: density (ρ = 8.96 g/cm^3), specific heat (Cp = 398 J/kgK), thickness (δ = 1.30 mm).

Table 1. Heat flux as a function of calorimeter position under plasma jet axis.

Calorimeter position *(mm)*	Heating rate *dT/dt (K/s)*	Deviation *(±K/s)*	Heat flux *(MW/m^2)*	Deviation *(±MW/m^2)*
40	467	10	2.18	0.05
60	292	8	1.37	0.04
80	192	8	0.90	0.04
100	138	6	0.65	0.03
120	97	6	0.45	0.03

The curve fitted to the experimental points (Fig. 6) give the heat flux equation as a function on the axial plasma jet position (Z) from the nozzle exit for plasma torch operating in default condition set for the tests: current (90.0 ± 0.9)A, voltage (345 ± 4)V, air flow (3.10 ± 0.03)g/s.

Therefore, according to Eq. (7), samples can be exposed to heat flux between 0.5 MWm^2 and 2.5 MWm^2, as a function on the axial plasma jet position (Z).

$$q_{cw} = \left(5,7\exp\left(-x/38\right)+0,23\right)MW/m^2 \tag{7}$$

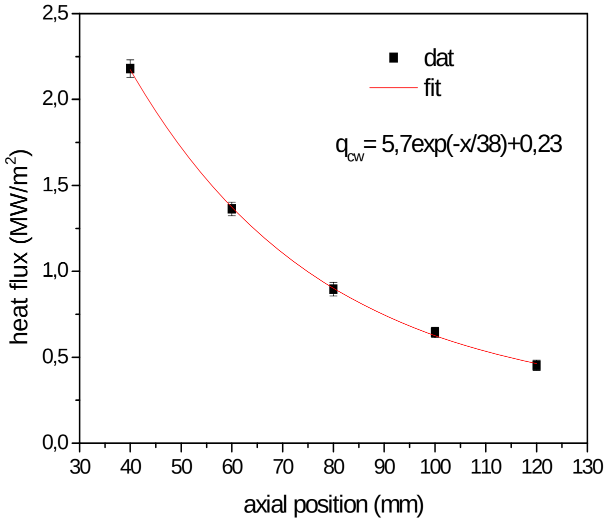

Figure 6. Heat flux (q_{cw}) transferred to the cold-wall calorimeter as a function on the axial plasma jet position (Z).

4.3. Samples tested with the jet plasma.

Figure 7 show quartz-phenolic composites sample, before and after exposure to the plasma jet. In the quartz-phenolic composite is observed the formation of a uniform carbonized layer in the exposed surface.

Figure 8 show carbon-phenolic composites sample, before and after exposure to the plasma jet. In carbon phenolic composites is observed that surface layer of resin was removed by exposure to the plasma jet, as the weft of the fabric-building became more apparent and dark.

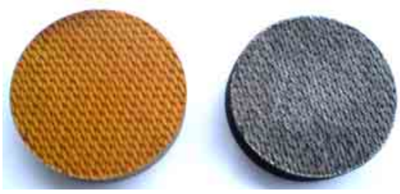

(a) (b)

Figure 7. Quartz-phenolic (*a*) before and (b) after exposure to the plasma jet.

(c) (d)

Figure 8. Carbon-phenolic (*a*) before and (b) after exposure to the plasma jet.

4.4. Scanning electron microscopy (SEM).

The Fig. 9 shows the SEM of quartz-phenolic composite after exposure to the plasma jet. In quartz-phenolic composite is observed that there was fusion of the most superficial layer of the fibers of quartz, since the melting temperature of the quartz is around 1500 ^{o}C.

The Fig. 10 shows the SEM of carbon-phenolic composite after exposure to the plasma jet. It is observed that there was only removing the resin, and there was no fusion of carbon fiber.

Figure 9. SEM quartz-phenolic after plasma jet exposure.

Figure 10. SEM carbon-phenolic after plasma jet exposure.

4.5. Sample temperatures.

The temperatures of samples were measured as described in Section 2.1.3, at surface with the optical pyrometer and inside with thermocouples inserted at 2 mm and 4 mm deep from the surface front. The samples were exposed to the heat flow (0.90 ± 0.04) MW/m^2 over 30s. The Fig. 11 (A) shows the graph of the surface and internal temperatures of quartz-phenolic composite, depending on time of exposure to the plasma jet and Fig. 11 (B) of the carbon phenolic composite. The measured temperatures in carbon-phenolic composite are higher than in quartz-phenolic composite, a difference greater than 100 ^{o}C, because the carbon fiber leading more heat (11W/mK) that the quartz fiber (1.5W/mK). Therefore, the quartz-phenolic composite shows a greater capacity of thermal insulation that carbon-phenolic composite.

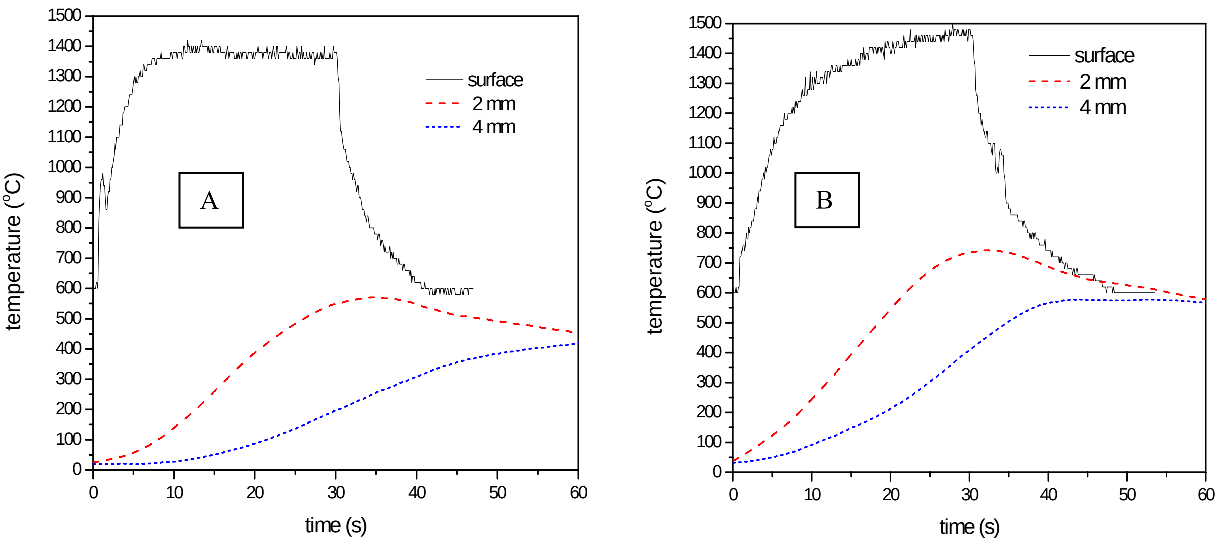

Figure 11. Sample temperature measured in surface and 2mm e 4mm deep as a function of plasma jet exposition time for composites (A) quartz-phenolic and (B) carbon-phenolic.

4.6. Sample massa loss.

The Fig. 12 shows the graph of the rate of weight loss, depending on the heat flux incident to quartz-phenolic composite and carbon phenolic samples. Observe that in both cases the rate of loss of mass increases with the heat flow incident.

The carbon phenolic composite shows rate of weight loss, about 25% higher than the quartz-phenolic composite. This is caused by the higher diffusivity of heat in the carbon phenolic composite, which occurs because of higher thermal conductivity of carbon fibers (11W/mK), which causes more fast volatilization and carbonization of phenolic resin and consequently, results in a greater mass loss, than for quartz fibers (1.5 W/mK).

4.7. Heat Ablation.

The Fig. 12 shows the graph of the heat of ablation, depending on the heat flux incident to quartz-phenolic composite and carbon phenolic samples. It is observed in both cases, the heat of ablation increases with the incident heat flux, and the carbon phenolic composite shows values 20% lower than the quartz-phenolic composite. This is caused by the increased loss of mass of carbon-phenolic composite, compared to the quartz-phenolic composite, as described in previous item. Linear fit of points on the graph give the Eq. (8) and Eq. (9) of the heat of ablation as a function of incident heat flux:

Composite quartz-phenolic: $$Q_{cw} = 9.6\ q_{cw} + 6.7 \quad (8)$$

Composite carbon-phenolic: $$Q_{cw} = 7.9\ q_{cw} + 4.5 \quad (9)$$

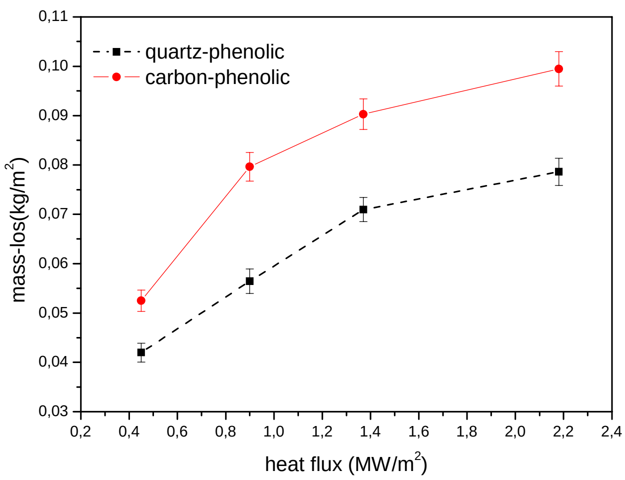

Figure 12. Mass loss of composite quartz-phenolic and carbon-phenolic as a function of heat flux.

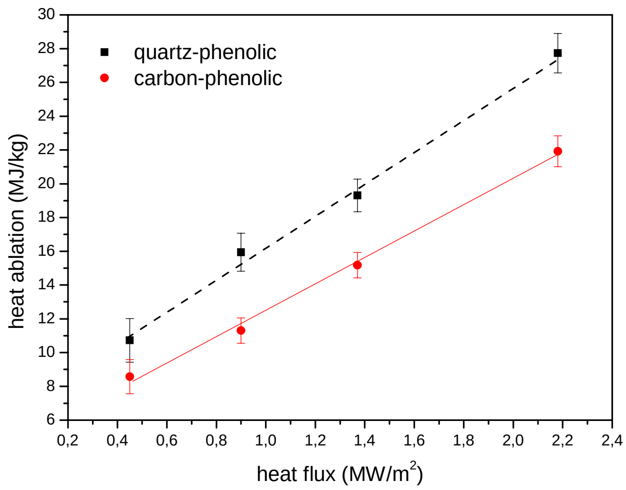

Figure 13. Heat of ablation of composite quartz-phenolic and carbon-phenolic as a function of heat flux.

5. CONCLUSIONS.

The plasma torch used was able to produces heat flux from 0.5MWm^2 to 2.5MWm^2, which are compatible than a high enthalpy flows expected in atmospheric reentry of an orbital vehicle. The intensity of heat flux from plasma jet as a function of axial position measured with cold wall calorimeter. What enables positioning and display samples of thermal protection material, the plasma jet produced by torch, as appropriate to determine the rate of removal of mass and heat of ablation of the material tested, depending on the heat flow and time of incident exposure.

Analyzing the experimental results it is concluded that among the samples of materials for thermal protection developed in the CTA, in the period 2007 2008, which were tested with the heat flux consistent with atmospheric reentry, between 0.5 MW/m^2 to 2.2 MW/m^2, the quartz-phenolic compound is what gives the greater degree of heat of ablation, compared to carbon-phenolic.

By SEM of quartz-phenolic composite finds that there was fusion of the superficial layer of the fibers of quartz-phenolic composite, because the melting temperature of the quartz is around 1500 ^{o}C, temperature that was reached during the test as results of the pyrometer measurements. Quartz fibers melting implies in a loss of mechanical strength of reinforcement composite. Therefore, in regions subject to mechanical strain, should consider the use of carbon fiber because of its melting temperature is around 3000 ^{o}C, temperatures well above those planned to be achieved during the reentry of an orbital vehicle.

The results obtained in carrying out this research make an essential criterion for qualification and certification of materials for thermal protection of aerospace, determining the heat of ablation of a material subjected to flow heat produced by a jet of plasma with the same intensity set for the atmospheric reentry of an orbital vehicle.

6. REFERENCES

Bahramian A. R., Kokabi, M. Famili, M. H. N. Beheshty, M. 2006. "Ablation and thermal degradation behaviour of a composite based on resol type phenolic resin: Process modeling and experimental". Polymer 47 (2006) 3661–3673 (www.elsevier.com/locate/polymer)

Charakhovski, L. I. ; SILVA, W. G. ; Essiptchouk, A. M. ; Pertraconi, G. ; Barros, E. A. ; MACIEL, H. S. ; Otani, C. . "Hypersonic and Subsonic Plasma Setups for Testing Heat Shielding Materials". In: 12th Brazilian Congress of Thermal Engineering and Sciences, 2008, Belo Horizonte. 12th Brazilian Congress of Thermal Engineering and Sciences. Rio de Janeiro : Proceedings of ENCIT 2008, 2008.

Fay, J. A., and Riddell, F. R., 1958, "Theory of Stagnation Point Heat Transfer in Dissociated Air" *Journal of Aeronautical Sciences*, Vol 25, No. 2, p. 73.

Lide, D.R. (Ed.), 2008, "CRC handbook of chemistry and physics: a ready-reference book of chemical and physical data". 88. ed. Boca Raton, FL: CRC, ISBN 0-8493-0488-1.

Ogasawara, T. and Ishikawa, T, 2002, "Thermal Response and Ablation Characteristics of Carbon Fiber Reiforced Composit with Novel silicon Containing Polymer MSP". Journal of composite material, vol 36, no 02.

Regan, F.J.; Anandakrishnan, S.M. 1993 "Dynamics of atmospheric re-entry**"**. Washington, DC: AIAA, (AIAA education series). ISBN 1 56347 048 9.

Schmidt, D.L., 1971, "Ablative Polymers in Aeroespace technology". In: ALELIO, G. F.; PARKER, J. A.; DEKKER, M. (ed.) Ablative plastics. New York, NY: ISBN 0-8247-1120-3.

7. RESPONSIBILITY NOTICE

The author is the only responsible for the printed material included in this paper.